Running head: IMMOBILIZATION-INDUCED BRAIN PLASTICITY

Title: Adaptive motor imagery: A multimodal study of immobilization-induced brain plasticity

Authors: Hana Burianová[1,2], Paul F. Sowman[2,3], Lars Marstaller[1,2,3], Anina N. Rich[2,3,5], Mark A. Williams[2,3,5], Greg Savage[2,4], Shahd Al-Janabi[2,3], Peter de Lissa[2,3], Blake W. Johnson[2,3]

[1]Centre for Advanced Imaging, University of Queensland, Brisbane, Australia
[2]ARC Centre of Excellence in Cognition and its Disorders, Macquarie University, Sydney, Australia
[3]Department of Cognitive Science, Macquarie University, Sydney, Australia
[4]Department of Psychology, Macquarie University, Sydney, Australia
[5]Perception in Action Research Centre, Faculty of Human Sciences, Macquarie University, Sydney, Australia

Correspondence should be addressed to:
Hana Burianová, PhD
Centre for Advanced Imaging
The University of Queensland,
Brisbane, QLD 4072, Australia
hana.burianova@cai.uq.edu.au

Pages: 26
Figures: 4

Abstract

The consequences of losing the ability to move a limb are traumatic. One approach that examines the impact of pathological limb non-use on the brain involves temporary immobilization of a healthy limb. Here, we investigated immobilization-induced plasticity in the motor imagery (MI) circuitry during hand immobilization. We assessed these changes with a multimodal paradigm, using fMRI to measure neural activation, MEG to track neuronal oscillatory dynamics, and TMS to assess corticospinal excitability. fMRI results show a significant decrease in neural activation for MI of the constrained hand, localized to sensorimotor areas contralateral to the immobilized hand. MEG results show a significant decrease in beta desynchronization and faster resynchronization in sensorimotor areas contralateral to the immobilized hand. TMS results show a significant increase in resting motor threshold in motor cortex contralateral to the constrained hand, suggesting a decrease in corticospinal excitability in the projections to the constrained hand. These results demonstrate a direct and rapid effect of immobilization on MI processes of the constrained hand, suggesting that limb non-use may not only affect motor execution, as evidenced by previous studies, but also MI. These findings have important implications for the effectiveness of therapeutic approaches that use MI as a rehabilitation tool to ameliorate the negative effects of limb non-use.

Keywords: Plasticity; Motor Imagery; Immobilization; Sensorimotor Cortex; Multimodal

Adaptive motor imagery: A multimodal study of immobilization-induced brain plasticity

Introduction

Limb non-use due to injury is known to induce considerable neural plasticity in the sensorimotor system, as has been demonstrated by studies that show reorganizational changes following pathological trauma, such as stroke (Liepert *et al*., 2000) or limb amputation (Lotze *et al*., 2001). To elucidate whether similar plastic changes occur in an intact nervous system, a number of research studies have utilized limb immobilization, a procedure that causes synaptic depression in sensorimotor regions (*e.g.,* Allen, Celikel, & Feldman, 2003). Typically, these studies examine changes in motor performance prior to and post immobilization, using motor execution (ME) tasks (Huber *et al*., 2006) or transcranial magnetic stimulation (TMS; Avanzino *et al.*, 2011). These studies have demonstrated deterioration in motor performance and changes in motor cortical excitability within days (Facchini *et al*., 2002) and even hours of immobilization (Avanzino *et al.*, 2011).

One technique proposed to be effective in mitigating the negative effects of limb non-use is motor imagery (MI; *e.g.,* Sharma, Pomeroy, and Baron, 2006). It has been argued that, due to the physiological similarities between ME and MI (Jeannerod, 2001), MI could be adopted in motor rehabilitation (Zimmermann-Schlatter *et al*., 2008). However, the assumption that MI would recruit the compromised motor pathways and thus ameliorate non-use induced changes proved unwarranted. The handful of controlled studies to date has yielded inconclusive or contradictory results (Crews & Kamen, 2006; Liu *et al.*, 2004; Page, Levine, & Leonard, 2005), indicating that using MI to stave off the deleterious effect of immobilization may be ineffective (Crews & Kamen, 2006).

Interestingly, while the effects of limb non-use on ME have been demonstrated in numerous studies, it has been presumed that MI remains unaffected (Johnson, 2000; Johnson *et al*., 2002). Yet, precisely *because* MI activates sensorimotor areas that overlap with those activated by ME (*e.g.,* primary motor cortex; Rossini *et al.*, 1999), it could be the case that the lack of somatosensory input and motor output that elicits reorganizational changes in the circuitry subserving the control of the immobilized hand also *directly* affects MI of movements of this hand.

The aim of this study was to investigate immobilization-induced plasticity during motor imagery by examining neural changes with functional magnetic resonance imaging (fMRI), changes in neural oscillatory dynamics with magnetoencephalography (MEG), and changes in corticospinal excitability with TMS. Based on the spatial information provided by fMRI, we used a virtual sensor approach to the MEG data, examining the temporal aspects of MI activation and their modulation by immobilization. Specifically, we investigated whether immobilization of the dominant hand would result in (i) a reduction of neural activity in the motor circuitry during MI of the immobilized hand; (ii) lateralization of immobilization-induced plasticity to sensorimotor regions contralateral to the immobilized hand; (iii) a change in the temporal signature of imagery-related desynchronization in the beta frequency band; and (iv) a change in the resting motor threshold in the motor cortex contralateral to the immobilized hand.

Based on the findings from previous studies that show a physiological overlap of ME and MI (Jeannerod, 2001; Nagakawa *et al*., 2011) and rapid immobilization-induced inter-hemispheric plasticity (Avanzino *et al*., 2011; Facchini *et al*., 2002), we predicted that 24-hour hand immobilization would result in a significant decrease in neural activity,

corticospinal excitability, and beta desynchronization in sensorimotor areas contralateral to the immobilized hand. Together with TMS, we used a finger-tapping task to directly measure the impact of rapid immobilization-induced plasticity on the speed of behavioural performance, predicting a significant increase in reaction times for the finger taps of the previously immobilized hand (Huber *et al*., 2006; Weibull *et al*., 2011). MI, an inherently an internal process, is notoriously difficult to measure behaviourally, typically relying on verbal report, indirect physiological measures, or more recently on experimenter-logged accuracy (Burianová *et al*., 2013a) or reaction times (Bassolino *et al*., 2013). In addition, finger or mouth responses are inappropriate during MI of hand movement, and thus we relied on accuracy of foot response after each MI sequence. This method ensured reliability of MI performance, but was not expected to change significantly post-immobilization.

Methods

Participants

Sixteen young adults (age range = 18-32; mean age = 26.1 years; SD = 4.3; 8 females) participated in the study. All participants were strongly right-handed (Oldfield, 1971), had normal or corrected-to-normal vision, and had no history of neurological impairment or psychiatric illness. All participants provided written informed consent approved by the Macquarie University Human Research Ethics Committee.

Experimental Design

The study consisted of three phases. In the first, *Pre-Immobilization Phase*, participants' brain activity was measured first by MEG, then by fMRI, whilst they

engaged in a finger configuration task, a recently developed paradigm that reliably invokes motor imagery (Burianová *et al*., 2013a). Following the scanning session, participants additionally engaged in a finger-tapping task, which allowed for a baseline measurement of efferent motor processes. In the second, *Immobilization Phase*, each participant's right forearm and hand was secured in a custom-moulded Aquaplast splint, bandaged from the elbow to the fingertips to prevent movement and sensory input, and carried in a sling. The arm and hand remained immobilized for 24 hours and throughout the follow-up MEG and fMRI sessions during which participants again performed the finger configuration task. Participants were instructed to not use their immobilized hand during the 24-hour delay and to perform routine actions, such as brushing teeth, with their left hand. To directly assess whether hand immobilization yielded non-correlational, quantifiable plastic changes in the brain, we measured the resting motor threshold (RMT) of the first dorsal interosseus muscle with TMS after each fMRI session of the study. Immediately after the Aquaplast splint was removed, participants again engaged in the finger-tapping task, in order to assess immobilization-induced effects on efferent motor processes.

Finger Tapping Task

This experimental paradigm consisted of visually cued (500ms), and regularly timed single finger tapping (500ms). Right finger taps were cued by centrally presented green square, whereas left finger taps were cued by centrally presented red square. We used a blocked design, with 16 index finger taps of each hand in sequence, 30 blocks in total. The participants were instructed to tap as quickly as possible to the visual cue. The order of conditions was counterbalanced across participants.

Finger Configuration Task

The details of this experimental paradigm are described elsewhere (Burianová *et al*., 2013a). In short, starting from a default position in which the arms rest alongside the body, with all fingers of the hand extended, participants heard a random sequence of 4 or 5 spoken digits (representing the fingers of the hand) and either (i) executed the movement – *i.e*., curl in or extend a specific finger, or (ii) imagined executing the movement. At the end of each cue sequence, participants saw a picture of a hand configuration and matched their own hand configuration to it by moving their right foot for "match" or left foot for "no match". For brevity, here we report data pertaining solely to the imagery conditions (Rimg and Limg). We used a blocked design, with four trials of each condition presented in sequence, followed by a 21-second block of rest, followed by the next condition. The order of conditions was randomized and counterbalanced across participants, but identical for MEG and fMRI. To confirm that participants were able to form mental images with sufficient vividness, they completed the Vividness of Visual Imagery Questionnaire (Marks, 1973). The range of the vividness scores was 51-73 (out of 80); mean score = 63.8; SD = 6.9.

Electromyographic (EMG) measurements were acquired during the MEG session to ensure that there was no muscle contraction during imagery trials. Two MEG compatible surface electrodes were attached to the *extensor digitorum* of each arm following the procedure described in Burgar, Valero-Cuevas, and Hentz (1997) and recorded using a BrainProducts MEG-compatible polygraphic system (BrainProducts GmbH, Gilching, Germany). EMG was acquired using a sampling rate of 1000 Hz and a filter bandpass of 20-500 Hz. We were unable to collect EMG data during the fMRI

session; instead, an experimenter observed participants' hands closely via a scanner camera throughout the scanning session to ensure that participants did not move their fingers during MI conditions.

fMRI & MEG Data Acquisition

Anatomical and functional magnetic resonance images were acquired at Macquarie University Hospital, Sydney, using a 3 Tesla Siemens Magnetom Verio scanner with a 12-channel head coil. Anatomical images were acquired using an MP-RAGE sequence (208 axial slices, TR = 2000 ms, TE = 3.94 s, FOV = 240 mm, voxel size = 0.9 mm^3, TI = 900, flip angle = 9º). Brain activation was assessed using the blood oxygenation level-dependent (BOLD) effect (Ogawa *et al.*, 1990) with optimal contrast. Functional images were obtained using a whole head T2*-weighted echo-planar image (EPI) sequence (40 axial slices with interleaved acquisition, 0.5 mm gap, TR = 3000 ms, TE = 30 ms, flip angle = 90º, FOV = 260 mm, voxel size = 2.5 mm^3).

MEG data were acquired at the KIT-Macquarie Brain Research Laboratory, Macquarie University, Sydney, using a 160-channel whole-head KIT system (Model PQ1160R-N2, Kanazawa, Japan) with first-order axial gradiometer sensors (50-mm baseline; Kado *et al*., 1999; Uehara *et al.*, 2003). Prior to MEG recordings, the 3D locations of three cardinal landmarks (the nasion and bilateral preauricular points), five marker coil positions, and head shape were measured with a pen digitizer (Polhemus Fastrack, Colchester, VT). Each subject's head position in relation to the sensors was measured at the start of each recording block using the five marker coils. A maximum threshold of 5 mm for any individual coil was set as movement tolerance. Continuous data were acquired using a sampling rate of 1000 Hz.

fMRI Preprocessing & Data Analysis

The acquired fMRI images were preprocessed using the Statistical Parametric Mapping software (SPM8; http://www.fil.ion.ucl.ac.uk/spm). The functional images were realigned onto the mean image for head-motion correction, the anatomical image was segmented and spatially normalized to the T1-weighted Montreal Neurological Institute (MNI) template, and the normalization parameters were applied to the functional data. Finally, the data were spatially smoothed by convolving each volume with an isotropic Gaussian kernel (FWHM = 6mm).

The procedure of the fMRI analysis was twofold, each addressing a specific hypothesis. First, we conducted a whole-brain analysis to compare neural activity between the *Pre-Immobilization* and *Immobilization Phases*, delineating reorganizational changes attributable to the immobilized hand. Second, we conducted a region-of-interest analysis in three *a priori* selected sensorimotor regions in each hemisphere - primary motor cortex (M1), premotor cortex (BA6), and primary somatosensory cortex (S1) - to examine whether or not, specifically within the sensorimotor system, the effects of immobilization are lateralized to the hemisphere contralateral to the immobilized hand.

Whole-Brain Analysis.

To examine modulation of whole-brain activity due to hand immobilization and its relation to the imagery conditions (Rimg and Limg) we used the multivariate method Partial Least Squares (PLS; McIntosh *et al*., 1996), which is designed to identify those groups of brain regions distributed over the entire brain whose activity changes as a function of task demands. The analytical steps of PLS (using the PLS software implemented in Matlab) are based on the assumption that cognition is the result of

integrated and coordinated activity of groups of brain regions (*i.e.*, distributed brain networks) rather than the independent activity of any single brain region. A detailed description of PLS can be found in Krishnan *et al.* (2011), but, in brief, PLS analysis uses singular value decomposition (SVD) of a single matrix that contains all participants' data to find a set of latent variables (LVs), which are mutually orthogonal dimensions that reduce the complexity of the data set. In other words, PLS decomposes the data to maximize the amount of covariance of an LV with respect to the experimental conditions. Thus, akin to Principal Component Analysis (PCA; *e.g.*, Friston, Frith, & Frackowiak, 1993), PLS enables us to differentiate the degree of contribution of different brain regions associated with task or performance. Each LV consists of a singular image of voxel saliences (*i.e.*, a spatiotemporal pattern of brain activity that reflects task-related changes or brain-behaviour correlations seen across conditions), a singular profile of task saliences (*i.e.*, a set of weights that indicate how brain activity in the singular image is expressed in each of the experimental conditions), and a singular value (*i.e.*, the amount of covariance accounted for by the LV). The first LV always accounts for the largest amount of covariance (*i.e.*, has the largest singular value), with subsequent LVs accounting for progressively smaller amounts. For each condition in each LV, we calculated summary measures of how strongly each participant expresses the particular pattern of activity seen on the LV. These measures, called brain scores, are the products of the weighted salience of each voxel and BOLD signals summed across the entire brain for each participant in each condition on a given LV. Salience indicates the degree to which a voxel is related to the LV and can be positive or negative, depending on the voxel's relation to the pattern of task-dependent differences identified by the LV. The

significance for each LV is determined by permutation tests (here we used 500 permutations) and the reliability of each brain voxel included in the pattern identified by the LVs is estimated by bootstrap resampling steps (here we used 100 bootstraps; Efron, 1985). Peak voxels with a bootstrap ratio (BSR; *i.e.*, salience/standard error) > 3.0 were considered to be reliable, as these approximate $p < 0.002$ (Sampson *et al.*, 1989).

Region-of-Interest Analysis.

To examine whether modulation of brain activity due to immobilization was lateralized to the hemisphere contralateral to the immobilized hand we used an ROI-based approach within three *a priori* selected somatosensory regions – M1, BA6, and S1 – in each hemisphere. We anatomically defined the ROIs, using the SPM Anatomy Toolbox (Eickhoff *et al*., 2005). Then, for each participant, we used MarsBar (Brett *et al*., 2002) to estimate the mean BOLD signal in each ROI from the preprocessed functional images using a general linear model with a standard hemodynamic response function for the contrasts Rimg > Fixation and Limg > Fixation. The results were thresholded at $p < 0.05$. The second-level (group) analyses of these results used a repeated-measures ANOVA on the mean activity in the ROIs, with factors Hemisphere (Left/Right) x Phase (Pre-Immob/Immob) x Condition (Rimg/Limg).

MEG Preprocessing & Data Analysis

MEG data were analyzed using Fieldtrip (Oostenveld *et al*., 2011) and SPM8. Data were downsampled to 250 Hz, filtered (bandpass 0.2-90 Hz), and epoched around the time of stimulus onset (-1000 to 2000ms). Artefacts including blinks and eye-movements were removed using the Fieldtrip artefact rejection tool implemented in SPM8. EMG traces from the arm were examined for every trial to ensure that there was

no overt activation during the imagery condition. Trials that had EMG activation during imagery conditions were excluded from the analysis. To calculate source lead fields, a canonical cortical mesh derived from the MNI template was warped, in a nonlinear manner, to match the participant's digitized head shape, and a forward model was computed using a single shell model.

Reconstructing source time courses

For the analysis, only ROIs within left and right BA6 and M1 were used, as it was expected that there would be significant overlap in the virtual sensor activity between S1 and M1 due to their close spatial location and the limited spatial selectivity of MEG. The time courses of source intensities for the four ROIs (radius 10mm) were reconstructed using a virtual sensor approach. Virtual sensor coordinates were based on the results of the fMRI experiment and defined as group average coordinates of the peak intensity voxel within the four ROIs (left and right BA6 and M1) across the two imagery conditions (Rimg and Limg) and phases (Pre-Immob and Immob). For each participant, time courses for each of the four virtual sensors were computed using a linearly constrained minimum variance (LCMV) spatial filter (0.1% regularization) for each of the four trial types (Condition x Phase). LCMV beamformer images were computed on a 5mm spaced grid defined in MNI space and restricted to points within the inner skull boundary. Values on the grid were interpolated using linear interpolation to produce volumetric images with 2mm resolution. The resulting data were then subjected to time-frequency analysis in order to examine the modulation of beta band activity induced by motor imagery.

Time-frequency analysis.

Time-frequency analysis was conducted on the single trial data for all virtual sensors in the frequency range between 2 and 40 Hz. Power was analyzed in 0.5 Hz steps using seven-cycle Morlet wavelets (Tallon-Baudry *et al*., 1996). Epochs were averaged within conditions and the resulting average epoch was cropped from -500 to 1500 ms and percentage change time–frequency responses were obtained by normalizing the entire epoch to the baseline (prestimulus period -500 to 0 ms). To assess statistically significant differences in the beta spectral profile over time, the beta envelope was calculated for each condition by averaging across the beta frequency band (13-30Hz), a cortical rhythm that is closely related to motor behaviours (Pfurtscheller & Lopes da Silva, 1999; Taniguchi *et al*., 2000). The resultant two-dimensional waveforms were compared within conditions across phase by non-parametric bootstrapping procedure (Delorme & Makeig, 2004; Manly, 1997) and corrected for multiple comparisons using the FDR method described by Benjamini and Yekutieli (2001).

TMS Analysis

Resting motor threshold of the first dorsal interosseus in both the left and right hands was measured prior to and during immobilization of the right hand. Responses were recorded (1000 x gain, bandpass filtered from 20-500Hz) from a bipolar electrode (Medi-Trace 100, Kendall/Tyco Healthcare, USA) montage. One electrode was placed over the muscle belly of the right first dorsal interosseus muscle and the other electrode was placed over the proximal metacarpal of the index finger. The resting motor threshold (RMT) for evoking a motor evoked potential in each muscle was determined using a Magstim 200 stimulator (The Magstim Co., Dyfed, UK) with a focal figure-of-eight coil, while the muscle was at rest. The coil was oriented 45° oblique to the sagittal mid-line

with the handle held posteriorly, so that the induced current flowed in a plane perpendicular to the estimated alignment of the central sulcus. RMT was determined at the first dorsal interosseus hotspot and defined as the intensity at which 5 out of 10 successive stimuli evoked an MEP with a peak-to-peak amplitude of at least 50 μV.

Results

Behavioural Performance

Finger Tapping Task.

The finger tapping task was used to examine direct motor changes associated with immobilization. Mean reaction times for visually cued left and right finger taps were analyzed using a Condition (Left Finger Tap/Right Finger Tap) x Phase (Pre-Immob/Post-Immob) repeated-measures ANOVA. Please note that taps under 100ms were excluded from the analysis. The analysis revealed a significant main effect of Condition: $F_{1,15} = 23.58$, $p < 0.001$, and a significant Condition x Phase interaction: $F_{1,15} = 45.03$, $p < 0.001$. The source of this interaction was revealed by paired-sample *t*-tests showing that both left and right finger taps differed significantly between the *Pre-Immobilization* and *Post-Immobilization Phases*, but in opposite directions. The left finger taps were significantly faster in the *Post-Immobilization Phase* compared to the *Pre-Immobilization Phase* ($p = 0.01$), whereas the right finger taps were significantly slower in the *Post-Immobilization Phase* compared to the *Pre-Immobilization Phase* ($p = 0.017$, **Fig 1**). In line with studies showing that deafferentiation of somatosensory input can result in decreased excitability in contralesional sensorimotor areas, and increased excitability and organizational changes in ipsilesional sensorimotor areas (Avanzino *et al*., 2011; Huber *et al*., 2006; Weibull *et al*., 2011), these results confirm that 24-hour

hand immobilization has a direct influence on efferent motor processes and thus on motor performance of both hands.

[Insert Figure 1 here]

Finger Configuration Task.

To assess performance on the finger configuration matching, two Condition (Limg/Rimg) x Phase (Pre-Immob/Immob) repeated-measures ANOVAs were conducted on the accuracy of responses during the MEG and fMRI sessions, respectively. The analyses revealed no significant main effect of Condition or Phase, and no significant Condition x Phase interaction (*p*s > 0.1), suggesting that configuration matching was consistent across the two testing sessions, regardless of hand immobilization.

TMS Results

Resting motor thresholds for the motor cortex contralateral to the immobilized hand were significantly increased during immobilization. Prior to immobilization (*Pre-Immobilization*) the RMT (mean ± SEM) for the right hand was 46.8 ± 1.6% of stimulator output. This threshold increased significantly ($p = 0.027$) to 51.3 ± 2.4% of stimulator output during *Immobilization*. There was no RMT change (47.4 ± 42.0% *Pre-Immobilization*; 47.3 ± 1.7% *Immobilization* ($p = 0.92$) in the motor cortex contralateral to the non-immobilized hand. Together with the results from the Finger Tapping Task, these results confirm that 24-hour hand immobilization directly affects activity in motor cortex contralateral to the constrained hand.

fMRI Results

Whole-Brain Multivariate Analyses.

To examine what impact immobilization has on the network of regions subserving MI, we analyzed the whole-brain data using PLS. The whole-brain analysis of the two imagery conditions and fixation between the *Pre-Immobilization* and *Immobilization Phases* for all participants yielded one significant LV, which accounted for 74% of covariance in the data ($p < 0.001$) and reflected a pattern of activity related to both motor imagery conditions in contrast to the fixation. This pattern included bilateral activations in M1, S1, basal ganglia, insula, cerebellum, inferior frontal gyrus, middle frontal gyrus, posterior parietal cortex, and superior temporal gyrus. Areas whose activity negatively correlated with the task conditions included left fusiform gyrus, right occipital gyrus, bilateral inferior parietal lobule, and posterior cingulate gyrus, reflecting the posterior nodes of the default mode network (*e.g.*, Buckner, Andrews-Hanna, and Schacter; 2008). To assess whether activity in each condition differed significantly between the two Phases, we conducted a second-level analysis of mean brain scores. A Condition (Rimg/Limg/Fix) x Phase (Pre-Immob/Immob) repeated-measures ANOVA revealed a significant main effect of Condition: $F_{2,14} = 35.59$, $p < 0.001$, a statistical trend of Phase: $F_{1,15} = 4.11$, $p = 0.062$, and a significant Condition x Phase interaction: $F_{2,14} = 5.99$, $p = 0.014$. Three paired-sample *t*-tests revealed that only activity during the right hand imagery condition differed significantly between the two phases, yielding significantly lower activation during the *Immobilization* than *Pre-Immobilization Phase* (M = 11.65, SD = 15.50; M = 22.72, SD = 19.59, $p = 0.004$, respectively; **Fig 2**). These results provide evidence that 24-hour hand immobilization has a direct influence on the neural circuitry that subserves MI of the immobilized hand.

[Insert Figure 2 here]

ROI Results.

To examine whether or not, specifically within the sensorimotor system, the effects of immobilization are lateralized to the hemisphere contralateral to the immobilized hand, we conducted an ROI analysis in three *a priori* selected sensorimotor regions in each hemisphere – M1, BA6, and S1. The analysis of the mean activity in M1 revealed a significant main effect of Hemisphere: $F_{1,15} = 17.13$, $p < 0.001$ and Phase: $F_{1,15} = 4.36$, $p = 0.050$, as well as significant interactions: Hemisphere x Phase: $F_{1,15} = 15.05$, $p = 0.002$, Hemisphere x Condition: $F_{1,15} = 11.40$, $p = 0.005$, and Hemisphere x Phase x Condition: $F_{1,15} = 9.00$, $p = 0.010$. *Post hoc* paired-sample *t*-tests (*p*-value Bonferroni-corrected for multiple comparisons) revealed that only during right-hand imagery the mean activity in left M1 was significantly lower in the *Immobilization Phase*, compared to the *Pre-Immobilization Phase* ($p = 0.003$; **Fig 3a**).

The analysis of the mean activity in BA6 revealed a significant main effect of Hemisphere: $F_{1,15} = 6.11$, $p = 0.027$ and significant interactions: Hemisphere x Phase: $F_{1,15} = 6.29$, $p = 0.025$, Hemisphere x Condition: $F_{1,15} = 8.68$, $p = 0.011$, and Hemisphere x Phase x Condition: $F_{1,15} = 9.18$, $p = 0.009$. *Post hoc* paired-sample *t*-tests (*p*-value Bonferroni-corrected for multiple comparisons) revealed that only during right-hand imagery the mean activity in left BA6 was significantly lower in the *Immobilization Phase*, compared to the *Pre-Immobilization Phase* ($p = 0.002$, Bonferroni-corrected for multiple comparisons; **Fig 3b**).

Finally, the analysis of the mean activity in S1 revealed a significant main effect of Phase: $F_{1,15} = 4.75$, $p = 0.047$ and significant interactions: Hemisphere x Condition: $F_{1,15} = 14.38$, $p = 0.002$ and Hemisphere x Phase x Condition: $F_{1,15} = 7.08$, $p = 0.019$.

However, none of the *post hoc t*-test comparisons were significant after Bonferroni-corrections (all $p > 0.050$; **Fig 3c**).

[Insert Figure 3 here]

MEG Results

Imagery of the finger movements elicited event-related desynchronization (ERD) in all four virtual MEG sensors within the canonical beta band (13-30Hz). The onset of beta ERDs in the imagery conditions began at around 300ms after the stimulus onset and peaked at around 600ms. Group statistical analysis of beta ERD envelopes showed a significant divergence between the *Pre-Immobilization* and *Immobilization Phases* for the right hand imagery condition. In the *Pre-Immobilization Phase*, maximum beta ERD was maintained at a plateau with a late resynchronization starting at around 1300ms, whereas in the *Immobilization Phase* an almost immediate resynchronization from maximum ERD began at around 700ms. This difference was evident in all virtual sensors but was statistically significant only for the left hemisphere sensors, *i.e.,* those contralateral to the constrained hand. There were no significantly different time bins between the *Pre-Immobilization* and *Immobilization Phases* in the right hemisphere M1 or BA6. Furthermore, there were no significant differences between the *Pre-Immobilization* and *Immobilization Phases* for the other imagery condition (Limg). In other words, there was a significantly earlier resynchronization in beta band oscillations only for MI of the immobilized hand and only within the ROIs in the hemisphere contralateral to the constrained hand (see **Fig 4**).

[Insert Figure 4 here]

Discussion

The objective of this study was to investigate neural plasticity of the human brain, specifically during motor imagery, following short-term hand immobilization. We used a multimodal paradigm to examine neural and oscillatory changes, as well as changes in corticospinal excitability. The behavioural results show direct effect of hand immobilization on the speed of efferent motor processes, and TMS results show direct evidence of immobilization effects via significantly increased resting motor thresholds in the motor cortex contralateral but not ipsilateral to the immobilized hand. fMRI results show that 24-hour hand immobilization leads to a significant decrease in neural activation during MI of the constrained hand, and this immobilization-induced plasticity was lateralized to sensorimotor areas (M1, S1, and BA6) contralateral to the immobilized hand. Finally, MEG results show a significantly faster resynchronization in the beta frequency band (*i.e.*, beta rebound) only for MI of the constrained hand. These effects are also localized to M1 and BA6 contralateral to the immobilized hand.

These results demonstrate first, that 24 hours of immobilization is sufficient to change the excitability of the relevant sensorimotor regions and modulate motor processes; and second, that this immobilization also affects the neural correlates of motor imagery. We saw specific changes in the recruitment of the contralateral sensorimotor cortex using both fMRI and MEG during motor imagery of the immobilized hand that were not due to general motor imagery effects or habituation. This direct and rapid effect on MI processes of a constrained hand suggests that limb non-use in general might affect both motor execution and imagery. The results have important therapeutic implications because health care practitioners increasingly use motor imagery as a rehabilitation tool to ameliorate the negative effects of limb non-use (Sharma *et al.*, 2006).

The current study shows the manner in which a multimodal approach can be used to provide complementary and convergent evidence for cortical changes induced by immobilization. The TMS and fMRI findings are in agreement with previous TMS studies that found decreased corticospinal excitability (Avanzino *et al*., 2013; Facchini *et al*., 2002; Kaneko *et al*., 2003), and fMRI studies that showed reduced activation in sensorimotor cortical areas following immobilization (Lissek *et al*., 2009). The temporal aspect of the MEG data reported here demonstrates the complementary value that can be added by using a highly temporally resolved method of neuroimaging in tandem with a highly spatially resolved method, *i.e.,* fMRI. Although the BOLD response derived from the fMRI experiment demonstrates that the activation of motor cortical areas is reduced by limb immobilization, the MEG data further elucidate the mechanisms by which immobilization reduces cortical activation mediated by MI.

The convergent findings of the current study suggest that short-term immobilization results in attenuated neural responses during MI that may reflect reduced specificity in cortical motor representations (*dedifferentiation*; Park *et al*., 2004). Dedifferentiation has typically been investigated in the context of ageing (*e.g*., Burianova *et al*., 2013b; St-Laurent *et al*., 2011), but has also been shown in cases in which excessive motor training led to focal dystonia (Byl *et al*., 1996), a deficiency in motor control associated with aberrant plasticity in the somatosensory cortex (Bara-Jimenez *et al*., 1998; Rosenkranz *et al*., 2009). Recently, researchers have established a relationship between beta band desynchronization and BOLD response in precentral cortex (Ritter *et al*., 2009), as well as a positive correlation between the strength of beta resynchronization and BOLD response in sensorimotor brain regions (Parkes *et al*., 2006). We suggest that

our results, showing decreased BOLD response in sensorimotor areas and earlier beta band resynchronization during MI of the immobilized hand, indicate an attenuated neural response in these brain regions. We further speculate that the observed neuronal attenuation during short-term immobilization is associated with reorganization of primary sensorimotor cortex and disturbance of proprioceptive-motor linkages (Avanzino *et al*., 2013). In line with Todorov (2004), we postulate that sensorimotor cortex provides proprioceptive feedback about the current position of the relevant limb during MI, which is important for the formation of appropriate internal models of movement (Shenton, Schwoebel, & Coslett, 2004), and that the results of the current study provide evidence of an attenuated sensorimotor activation due to reduced proprioceptive reafference during immobilization.

Two methodological limitations need to be stressed. Firstly, rather than the VVIQ (Marks, 1973), a more specific assessment of the ability to imagine motor movements would have been, for instance, the Movement Imagery Questionnaire (Hall & Martin, 1997). Our goal was to ensure a high degree of imagery vividness *per se*, which the VVIQ measures sufficiently. In addition, participants underwent extensive motor imagery training prior to the scanning session, as discussed in our previous work (Burianová *et al*., 2013a), to ensure familiarization with the task and the required imagery of motor movements. Secondly, despite recent advances in attaining a more precise index of MI performance (Burianová *et al*., 2013a, Bassolino *et al*., 2013), in addition to measuring MI accuracy, the study would benefit from a measure of MI speed (via *e.g.,* MRI-compatible foot pedals), which would allow a direct comparison with the behavioural index of motor execution on the finger-tapping task and which, we speculate, would

show similar swift post-immobilization changes, in line with the multimodal evidence at the neural level.

In conclusion, the findings of the current study have important implications for therapeutic practitioners who utilize MI as a rehabilitative tool for *e.g.,* stroke recovery. Proponents of MI therapy posit that, unlike motor execution, MI does not rely on residual sensorimotor function (Sharma *et al*., 2006), and further suggest that only lesions in parietal cortices would directly affect MI, as evidenced by a reduction in MI accuracy in a single patient with parietal damage (Tomasino *et al*., 2003). However, the results of this comprehensive study, utilizing two different neuroimaging methods and neural stimulation, demonstrate that limb immobilization directly affects the sensorimotor cortices that represent the restricted limb, suggesting that representations critical for MI are affected by limb non-use. Our findings support the notion that imagery may not be effective in ameliorating disuse-related deficits (Crews & Kamen, 2006), at least immediately after injury. Further investigations are necessary to establish the longitudinal course of neuroplasticity underlying the MI circuitry.

Acknowledgements: The authors would like to thank all participants for their time and effort in this multimodal monster of a study. This work was funded by the National Health and Medical Research Council (NHMRC). The authors declare no competing financial interests.

Figure Captions

FIG 1. Performance on the Finger Tapping Task. Mean reaction times for left index finger (left bars) and right index finger (right bars) taps. Significance in all figures is denoted by '*'.

FIG 2. fMRI Whole-Brain Results: (a) A pattern of whole-brain activity depicting areas active during imagery conditions (yellow/red) *vs.* fixation (blue/green). **(b)** Brain scores related to whole-brain activity seen in (a) across the three conditions and two phases. Error bars denote 95% confidence intervals for correlations calculated from the bootstrap procedure.

FIG 3. fMRI ROI Results: (a) M1; **(b)** BA6; **(c)** S1 activation during right hand imagery pre-immobilization (blue bars) and during immobilization (red bars). Error bars denote standard error.

FIG 4. MEG Results: Effects of hand immobilization on event-related desynchronization (ERD) in the beta frequency band (13-30 Hz) in left and right M1. Time-frequency plots (on the left) show a reduced ERD and power envelopes (on the right) show a significantly earlier beta-synchronization (grey area) in left M1 contralateral to the immobilized hand.

References

Allen, C. B., Celikel, T., & Feldman, D. E. (2003). Long-term depression induced by sensory deprivation during cortical map plasticity in vivo. *Nature Neuroscience, 6*, 291-299.

Avanzino, L., Bassolino, M., Pozzo, T., & Bove, M. (2011). Use-dependent hemispheric balance. *Journal of Neuroscience, 31*, 3423-3428.

Avanzino, L., Pelosin, E., Abbruzzese, G., Bassolino, M., Pozzo, T., & Bove, M. (2013). Shaping motor cortex plasticity through proprioception. *Cerebral Cortex*. doi: 10.1093/cercor/bht139.

Bara-Jimenez, W., Catalan, M.J., Hallett, M. & Gerloff, C. (1998). Abnormal somatosensory homunculus in dystonia of the hand. *Annals of Neurology*, *44*, 828-831.

Bassolino, M., Campanella, M., Bove, M., Pozzo, T. & Fadiga, L. (2013). Training the motor cortex by observing the actions of others during immobilization. Cerebral Cortex, doi: 10.1093/cercor/bht190.

Benjamini, Y., & Yekutieli, D. (2001). The control of the false discovery rate in multiple testing under dependency. *Annals of Statistics, 29*, 1165-1188.

Brett, M., Anton, J.-L., Valabregue, R. & Poline, J.-B. (2002). Region of interest analysis using an SPM toolbox [abstract]. Presented at the 8th International Conference on Functional Mapping of the Human Brain, Sendai, Japan. Available on CD-ROM in *NeuroImage*, 16(2).

Buckner, R. L., Andrews-Hanna, J. R., & Schacter, D. L. (2008). The brain's default network - Anatomy, function, and relevance to disease. *Year in Cognitive Neuroscience 2008, 1124*, 1-38.

Burgar, C. G., Valero-Cuevas, F. J., & Hentz, V. R. (1997). Fine-wire electromyographic recording during force generation - Application to index finger kinesiologic studies. *American Journal of Physical Medicine & Rehabilitation, 76*, 494-501.

Burianova, H., Marstaller, L., Sowman, P., Tesan, G., Rich, A. N., Williams, M., Maruff, P., Baker, C., Savage, G. & Johnson, B. W. (2013a). Multimodal functional imaging of motor imagery using a novel paradigm. *Neuroimage, 71*, 50-58.

Burianova, H., Lee, Y., Grady, C.L. & Moscovitch, M. (2013b). Age-related dedifferentiation and compensatory changes in the functional network underlying face processing. *Neurobiology of Aging*, *34*, 2759-2767.

Byl, N.N., Merzenich, M.M. & Jenkins, W.M. (1996). A primate genesis model of focal dystonia and repetitive strain injury. *Neurology*, *47*, 508-520.

Crews, R. T., & Kamen, G. (2006). Motor-evoked potentials following imagery and limb disuse. *International Journal of Neuroscience, 116*, 639-651.

Delorme, A., & Makeig, S. (2004). EEGLAB: an open source toolbox for analysis of single-trial EEG dynamics including independent component analysis. *Journal of Neuroscience Methods, 134*, 9-21.

Efron, B. (1985). Bootstrap Confidence-intervals for a class of parametric problems. *Biometrika, 72*, 45-58.

Eickhoff, S. B., Stephan, K. E., Mohlberg, H., Grefkes, C., Fink, G. R., Amunts, K., & Zilles, K. (2005). A new SPM toolbox for combining probabilistic cytoarchitectonic maps and functional imaging data. *Neuroimage, 25*, 1325-1335.

Facchini, S., Romani, M., Tinazzi, M., & Aglioti, S. M. (2002). Time-related changes of excitability of the human motor system contingent upon immobilisation of the ring and little fingers. *Clinical Neurophysiology, 113*, 367-375.

Friston, K.J., Frith, C. & Frackowiak, R.S.J. (1993). Principal component analysis learning algorithms: A neurobiological analysis. *Proceedings of the Royal Society B*, *25*4, 47-54.

Hall, C. & Martin, K.A. (1997). Measuring movement imagery abilities: A revision of the Movement Imagery Questionnaire. *Journal of Mental Imagery*, *21*, 143-154.

Huber, R., Ghilardi, M. F., Massimini, M., Ferrarelli, F., Riedner, B. A., Peterson, M. J., & Tononi, G. (2006). Arm immobilization causes cortical plastic changes and locally decreases sleep slow wave activity. *Nature Neuroscience, 9*, 1169-1176.

Jeannerod, M. (2001). Neural simulation of action: A unifying mechanism for motor cognition. *Neuroimage, 14*, S103-S109.

Jonson, S.H. Imagining the impossible: Intact motor representations in hemiplegics. (2000). *Neuroreport*, *11*, 729-732.

Johnson, S.H., Sprehn, G. & Saykin, A.J. (2002). Intact motor imagery in chronic upper limb hemiplegics: Evidence for activity-independent action representations. *Journal of Cognitive Neuroscience*, *14*, 841-852.

Kado, H., Higuchi, M., Shimogawara, M., Haruta, Y., Adachi, Y., Kawai, J., . . . Uehara, G. (1999). Magnetoencephalogram systems developed at KIT. *Ieee Transactions on Applied Superconductivity, 9*, 4057-4062.

Kaneko, K., Taguchi, T., Yonemura, H., Ueno, H., Li, Z., & Kawai, S. (2003). Does cortical motor neuron excitability change in peripheral nerve injury? *Clinical Neurophysiology, 114*, 596-599.

Krishnan, A., Williams, L. J., McIntosh, A. R., & Abdi, H. (2011). Partial Least Squares (PLS) methods for neuroimaging: A tutorial and review. *Neuroimage, 56*, 455-475.

Liepert, J., Bauder, H., Wolfgang, H. R., Miltner, W. H., Taub, E., & Weiller, C. (2000). Treatment-induced cortical reorganization after stroke in humans. *Stroke, 31*, 1210-1216.

Lissek, S., Wilimzig, C., Stude, P., Pleger, B., Kalisch, T., Maier, C., . . . Dinse, H. R. (2009). Immobilization Impairs Tactile Perception and Shrinks Somatosensory Cortical Maps. *Current Biology, 19*, 837-842.

Liu, K. P., Chan, C. C., Lee, T. M., & Hui-Chan, C. W. (2004). Mental imagery for promoting relearning for people after stroke: A randomized controlled trial. *Archives of Physical Medicine and Rehabilitation, 85*, 1403-1408.

Lotze, M., Flor, H., Grodd, W., Larbig, W., & Birbaumer, N. (2001). Phantom movements and pain - An MRI study in upper limb amputees. *Brain, 124*, 2268-2277.

Manly, B. F. J. (1997). Randomization, bootstrap, and Monte Carlo methods in biology (2nd ed.). London: Chapman & Hall.

Marks, D. F. (1973). Visual-imagery differences and eye-movements in recall of pictures. *Perception & Psychophysics, 14*, 407-412.

McIntosh, A. R., Bookstein, F. L., Haxby, J. V., & Grady, C. L. (1996). Spatial pattern analysis of functional brain images using partial least squares. *Neuroimage, 3*, 143-157.

Nagakawa, K., Aokage, Y., Fukuri, T., Kawahara, Y., Hashizume, A., Kurisu, K. & Yuge, L. (2011). Neuromagnetic beta oscillation changes during motor imagery and motor execution of skilled movements. *Neuroreport*, *22*, 217-222.

Ogawa, S., Lee, T. M., Kay, A. R., & Tank, D. W. (1990). Brain magnetic-resonance-imaging with contrast dependent on blood oxygenation. *Proceedings of the National Academy of Sciences, U S A, 87*, 9868-9872.

Oldfield, R.C. (1971). The assessment and analysis of handedness: the Edinburgh inventory. *Neuropsychologia*, *9*, 97–113.

Oostenveld, R., Fries, P., Maris, E., & Schoffelen, J. M. (2011). FieldTrip: Open source software for advanced analysis of MEG, EEG, and invasive electrophysiological data. *Computational Intelligence and Neuroscience, 2011*, 156869.

Page, S. J., Levine, P., & Leonard, A. C. (2005). Effects of mental practice on affected limb use and function in chronic stroke. *Archives of Physical Medicine and Rehabilitation, 86*, 399-402.

Park, D.C., Polk, T.A., Park, R., Minear, M., Savage, A. & Smith, M.R. (2004). Aging reduces neural specialization in ventral visual cortex. *Proceedings of the National Academy of Sciences*, *101*, 13091-13095.

Parkes, L.M., Bastiaansen, M.C.M. & Norris, D.G. (2006). Combining EEG and fMRI to investigate the post-movement beta rebound. *NeuroImage*, *29*, 685-696.

Pfurtscheller, G., & Lopes da Silva, F. H. (1999). Event-related EEG/MEG synchronization and desynchronization: basic principles. *Clinical Neurophysiology, 110*, 1842-1857.

Ritter, P., Moosmann, M. & Villringer, A. (2009). Rolandic alpha and beta EEG rhythms' strengths are inversely related to fMRI-BOLD signal in primary somatosensory and motor cortex. *Human Brain Mapping*, *30*, 1168-1187.

Rossini, P. M., Rossi, S., Pasqualetti, P., & Tecchio, F. (1999). Corticospinal excitability modulation to hand muscles during movement imagery. *Cerebral Cortex, 9*, 161-167.

Rosenkranz, K., Butler, K., Williamon, A. & Rothwell, J.C. (2009). Regaining motor control in musician's dystonia by restoring sensorimotor organization. *Journal of Neuroscience*, *29*, 14627-14636.

Sampson, P. D., Streissguth, A. P., Barr, H. M., & Bookstein, F. L. (1989). Neuro-behavioral effects of prenatal alcohol: part II. Partial least-squares analysis. *Neurotoxicology and Teratology, 11*, 477-491.

Sharma, N., Pomeroy, V. M., & Baron, J. C. (2006). Motor imagery - A backdoor to the motor system after stroke? *Stroke, 37*, 1941-1952.

Shenton, J. T., Schwoebel, J., & Coslett, H. B. (2004). Mental motor imagery and the body schema: evidence for proprioceptive dominance. *Neuroscience Letters, 370*, 19-24.

St-Laurent, M., Abdi, H., Burianová, H. & Grady, C. (2011). Influence of aging on the neural correlates of autobiographical, episodic, and semantic memory retrieval. J*ournal of Cognitive Neuroscience*, *23*, 4150-4163.

Tallon-Baudry, C., Bertrand, O., Delpuech, C., & Pernier, J. (1996). Stimulus specificity of phase-locked and non-phase-locked 40 Hz visual responses in human. *Journal of Neuroscience, 16*, 4240-4249.

Taniguchi, M., Kato, A., Fujita, N., Hirata, M., Tanaka, H., Kihara, T., . . . Yoshimine, T. (2000). Movement-related desynchronization of the cerebral cortex studied with spatially filtered magnetoencephalography. *Neuroimage, 12*, 298-306.

Todorov, E. (2004). Optimality principles in sensorimotor control. *Nature Neuroscience*, *7*, 907-915.

Tomasino, B., Rumiati, R.I. & Umilta, C.A. (2003). Selective deficit of motor imagery as tapped by a left-right decision of visually presented hands. *Brain & Cognition*, *53*, 376-380.

Uehara, G., Adachi, Y., Kawai, J., Shimogawara, M., Higuchi, M., Haruta, Y., . . . Kado, H. (2003). Multi-channel SQUID systems for biomagnetic measurement. *Ieice Transactions on Electronics, E86c*, 43-54.

Weibull, A., Flondell, M., Rosen, B. & Bjorkman, A. (2011). Cerebral and clinical effects of short-term hand immobilisation. *European Journal of Neuroscience*, *33*, 699-704.

Zimmermann-Schlatter, A., Schuster, C., Puhan, M. A., Siekierka, E., & Steurer, J. (2008). Efficacy of motor imagery in post-stroke rehabilitation: a systematic review. *Journal of Neuroengineering and Rehabilitation, 5*. doi: Artn 8

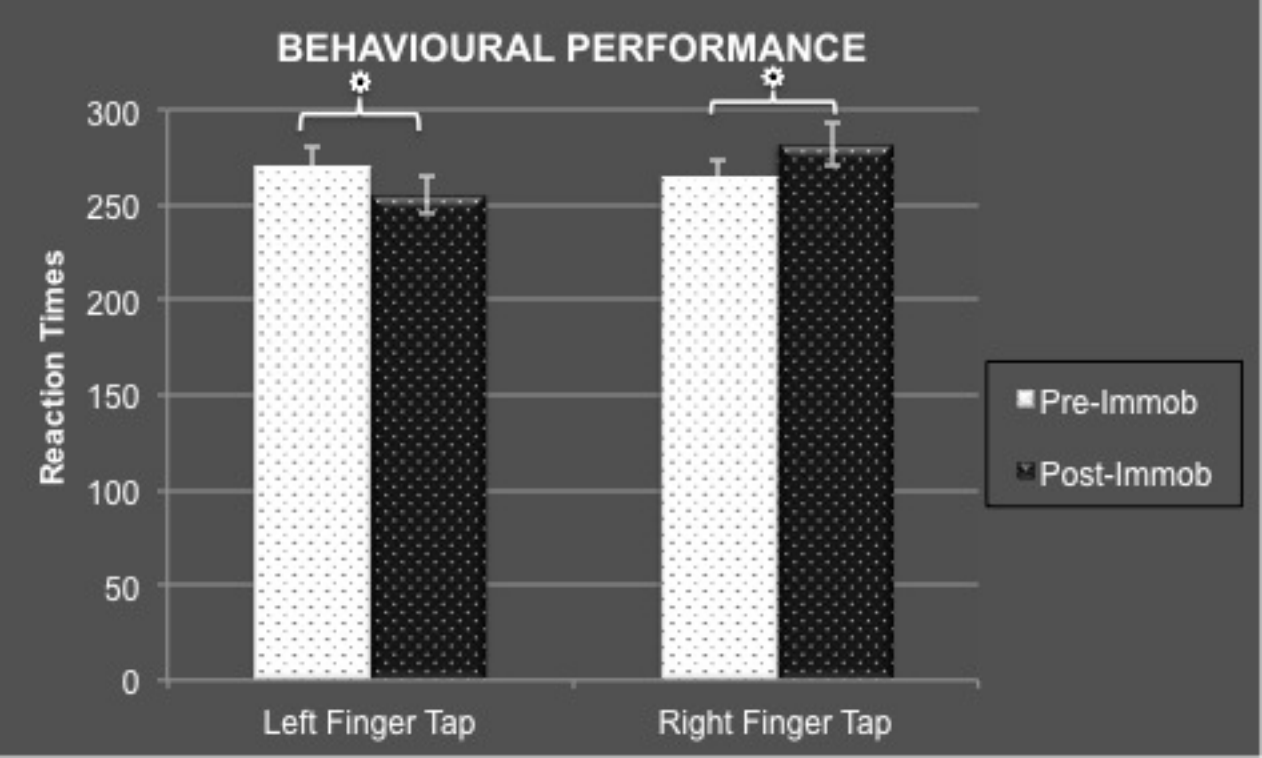
BEHAVIOURAL PERFORMANCE
Reaction Times
300
250
200
150
100
50
0
Left Finger Tap
Right Finger Tap
Pre-Immob
Post-Immob

a)

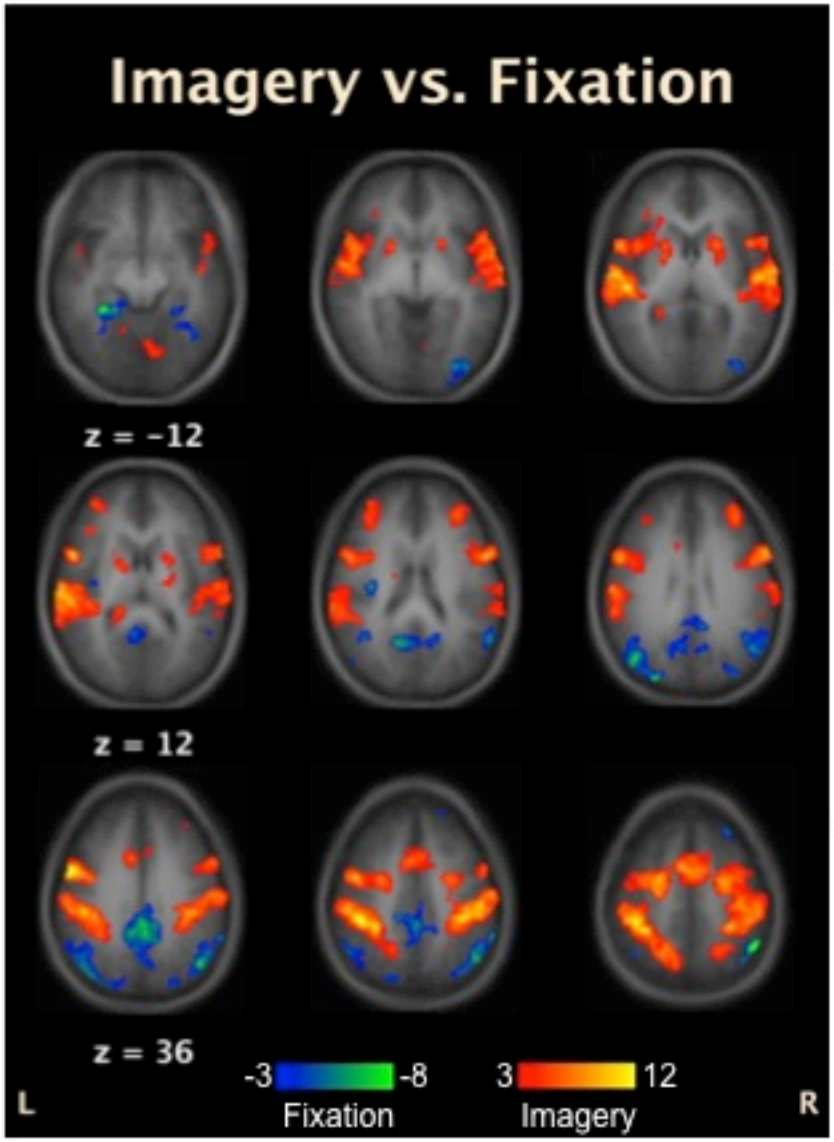
Imagery vs. Fixation
z = −12
z = 12
z = 36
-3
-8
Fixation
3
12
Imagery
L
R

b)

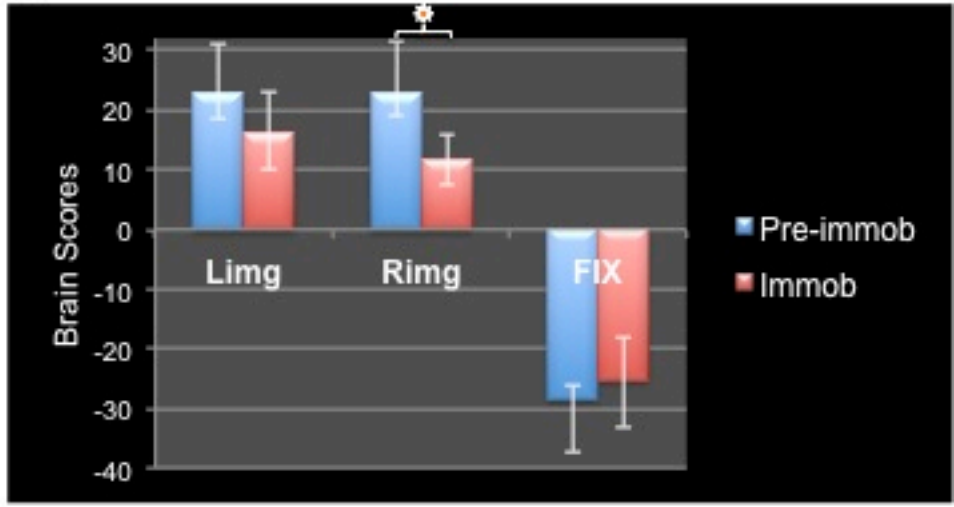
Brain Scores
30
20
10
0
-10
-20
-30
-40
Limg
Rimg
FIX
Pre-immob
Immob

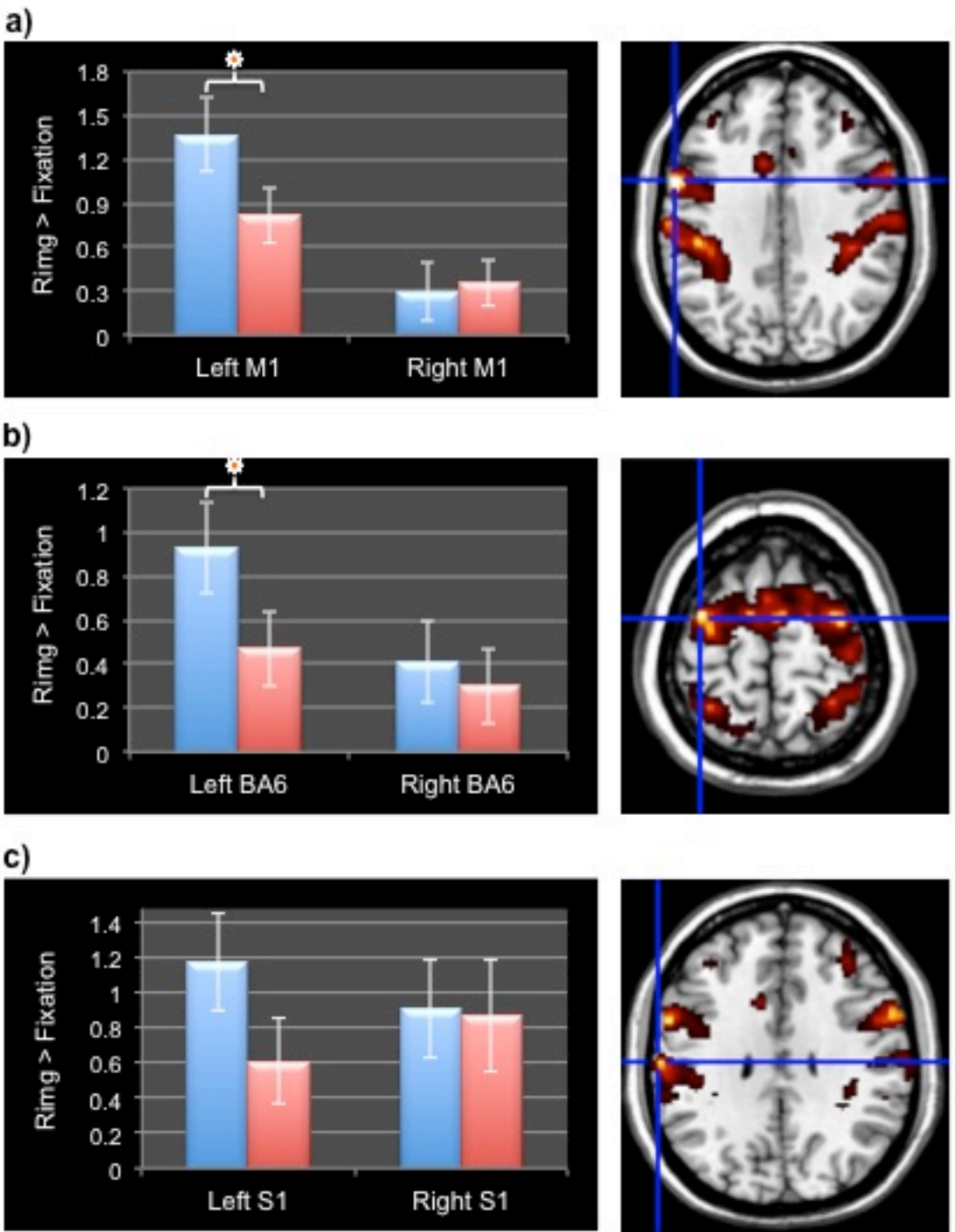
a)
Rimg > Fixation
1.8
1.5
1.2
0.9
0.6
0.3
0
Left M1
Right M1
b)
Rimg > Fixation
1.2
1
0.8
0.6
0.4
0.2
0
Left BA6
Right BA6
c)
Rimg > Fixation
1.4
1.2
1
0.8
0.6
0.4
0.2
0
Left S1
Right S1
Pre-immob
Immob

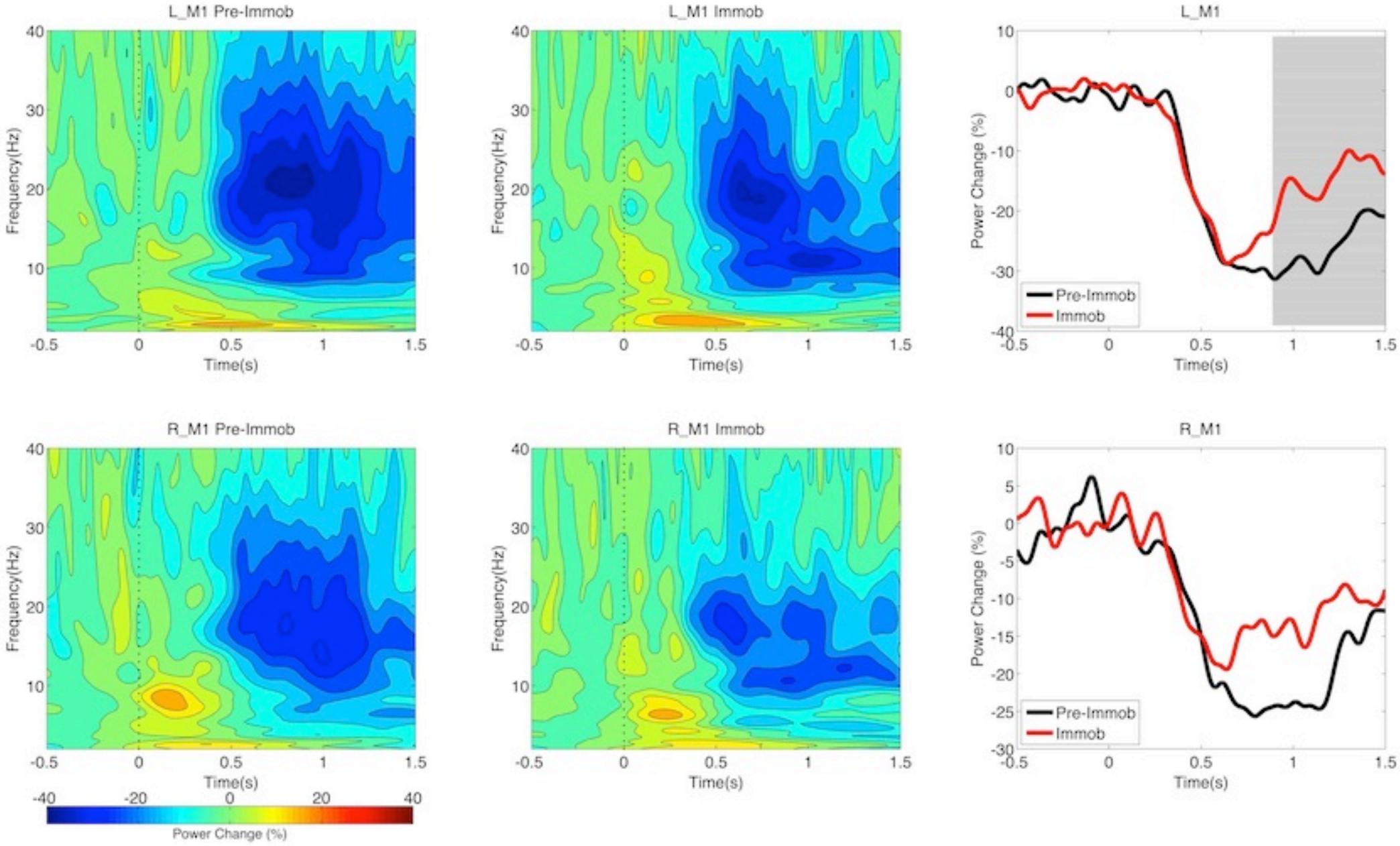
L_M1 Pre-Immob
L_M1 Immob
L_M1
R_M1 Pre-Immob
R_M1 Immob
R_M1
Frequency(Hz)
Time(s)
Power Change (%)
Pre-Immob
Immob
-40
-20
0
20
40
Power Change (%)